



OPEN ACCESS

EDITED BY

Fajin Chen,
Guangdong Ocean University, China

REVIEWED BY

Jianghu Lan,
Institute of Earth Environment (CAS),
China
Guoqiang Li,
Lanzhou University, China

*CORRESPONDENCE

Zhongping Lai
zhongping_lai@stu.edu.cn

SPECIALTY SECTION

This article was submitted to
Marine Biogeochemistry,
a section of the journal
Frontiers in Marine Science

RECEIVED 29 August 2022

ACCEPTED 17 October 2022

PUBLISHED 03 November 2022


CITATION

Zhong J, Ling K, Yang M, Shen Q,
Abbas M and Lai Z (2022) Radiocarbon
and OSL dating on cores from the
Chaoshan delta in the coastal South
China Sea.
Front. Mar. Sci. 9:1030841.
doi: 10.3389/fmars.2022.1030841

COPYRIGHT

© 2022 Zhong, Ling, Yang, Shen, Abbas
and Lai. This is an open-access article
distributed under the terms of the
[Creative Commons Attribution License
\(CC BY\)](https://creativecommons.org/licenses/by/4.0/). The use, distribution or
reproduction in other forums is
permitted, provided the original
author(s) and the copyright owner(s)
are credited and that the original
publication in this journal is cited, in
accordance with accepted academic
practice. No use, distribution or
reproduction is permitted which does
not comply with these terms.

Radiocarbon and OSL dating on cores from the Chaoshan delta in the coastal South China Sea

Jiemei Zhong¹, Ken Ling², Meifei Yang³, Qinjing Shen¹,
Mahmoud Abbas ¹ and Zhongping Lai^{1,4*}

¹Institute of Marine Sciences, Guangdong Provincial Key Laboratory of Marine Disaster Prediction and Prevention, Shantou University, Shantou, China, ²Guangdong Geological Survey Institute, Guangzhou, China, ³School of Earth Sciences, China University of Geosciences, Wuhan, China, ⁴Southern Marine Science and Engineering Guangdong Laboratory (Zhuhai), Zhuhai, China

Accurate chronology plays a crucial role in reconstructing delta evolution. Radiocarbon (¹⁴C) and optically stimulated luminescence (OSL) dating are widely used to establish a stratigraphic chronology of the late Quaternary sediments. The Chaoshan plain is located on the southern coast of China and borders the South China Sea. The thickness of Quaternary sediments in this area extends to a depth of 140 m and is considered a valuable archive for studying the evolution of the delta in response to climate and sea-level changes. However, reliable chronological data are still very limited. In this paper, eighteen accelerator mass spectrometry (AMS) ¹⁴C and thirteen quartz OSL ages were obtained from two cores from the Rongjiang plain, the middle part of the Chaoshan plain: ZK001 (90.85 m in depth) and ZK002 (100 m in depth). The present study aims to provide a reliable chronology of the Chaoshan plain based on OSL and ¹⁴C dating methods and examine the upper limit of the ¹⁴C dating on plant remains. Our results show that (1) OSL ages of cores ZK001 and ZK002 range from 56 to 1.7 ka and from 177 to 15 ka, respectively; (2) ¹⁴C ages of core ZK002 range from 8.8 to 41 cal ka BP, showing that all ¹⁴C ages below ca. 30 m depth are younger than OSL ages and that the upper limit of plant remains is around 35 cal ka BP. OSL ages are consistent with stratigraphic order within uncertainties. The oldest OSL age obtained from core ZK002 is 177 ± 20 ka at a depth of 93 m, and is considered a minimum age. This indicates that the Quaternary deposition in the Rongjiang plain can trace back to at least the marine isotope stage (MIS) 6 during sea-level lowstand, during which the plain is mainly influenced by the fluvial process. The comparison between ¹⁴C and OSL ages in the Chaoshan plain suggests that ¹⁴C ages older than 35 cal ka BP need to be re-evaluated. However, the OSL dating method proves reliable for establishing a comprehensive chronological framework for the late Quaternary sediments in this area.

KEYWORDS

¹⁴C ages of plant remains, OSL dating, estuary sediments, Chaoshan plain, South China Sea

Introduction

Robust chronology is essential for reconstructing the late Quaternary evolution in the delta environment. The radiocarbon dating method is regarded as a reliable dating method with an age limit, theoretically, up to approximately 55,000 years (Hajdas et al., 2021). However, a growing number of geochronologic studies corroborated that the reliability of radiocarbon dating for late Pleistocene sediments is problematic due to the age limit cluster around 35–40 ka BP (Yim et al., 1990; Pigati et al., 2007; Yi et al., 2013; Wang et al., 2018a; Miller and Andrews, 2019; Agatova et al., 2020; Al-Saqarat et al., 2021), or approximately 25 ka BP in practice (Lai et al., 2014; Wang et al., 2014; Song et al., 2015; Li et al., 2020c; Cheng et al., 2022; Long et al., 2022). The optically stimulated luminescence (OSL) dating method has become widely accepted in recent decades, with its merits of a long time-scale range (even up to 200 ka) and abundance of dating materials (e.g., quartz or feldspar) (Murray and Olley, 2002; Rhodes, 2011; Murray et al., 2021). The applicability of OSL dating to coastal and marine sediments allowed the reconstruction of the paleoenvironment of the delta (Chen et al., 2010; Guo et al., 2013; Yi et al., 2013; Wang et al., 2016; Xu et al., 2020; Gao et al., 2021; Long et al., 2022; Xu et al., 2022).

The Chaoshan plain is located on the eastern coast of Guangdong province (Figure 1). The Quaternary sediments in this area reach a depth of up to approximately 140 m, providing valuable archives for understanding the evolution of the delta in response to climate and sea level changes (Li et al., 1987; Wang

et al., 1997; Song et al., 2012). Due to the actual detection age limit of the ^{14}C dating method, most of the late Pleistocene chronology of the Chaoshan plain is disputed (Li et al., 1987; Zong, 1987; Li et al., 1988; Sun et al., 2007). Some studies have demonstrated that the oldest Quaternary deposits (fluvial sediments, named the Nanshe Formation) do not exceed 55 ka BP, based on radiocarbon, thermoluminescence (TL) dating, and stratigraphic relationships (Chen, 1984a; Li et al., 1987; Zong, 1987; Li et al., 1988; Sun et al., 2007; Zhou, 2008). Nevertheless, results from other dating methods, including electron spin resonance (ESR) and OSL, have shown that the oldest Quaternary sediments in the Lianjiang plain, the southeastern part of the Chaoshan plain, date back to more than 260 ka (Song et al., 2012; Tang et al., 2018). Yet, our understanding of the formation and evolution of the Chaoshan plain delta is still debated, owing to different dating methods that require further evaluation. A direct comparison between different dating techniques applied to the basal Quaternary deposits would help to answer this question.

In this study, Quaternary estuarine sediments from two cores, ZK001 with a depth of 90.85 m and ZK002 with a depth of 100 m, in the Chaoshan plain were dated using ^{14}C and OSL dating methods. We aim to understand the delta evolution and address the following issues: (1) examining the reliability of ^{14}C and OSL dating by mutual verification; (2) exploring the practical detection limit of ^{14}C dating using plant remains; and (3) determining the age of onset of Quaternary deposition in the area.

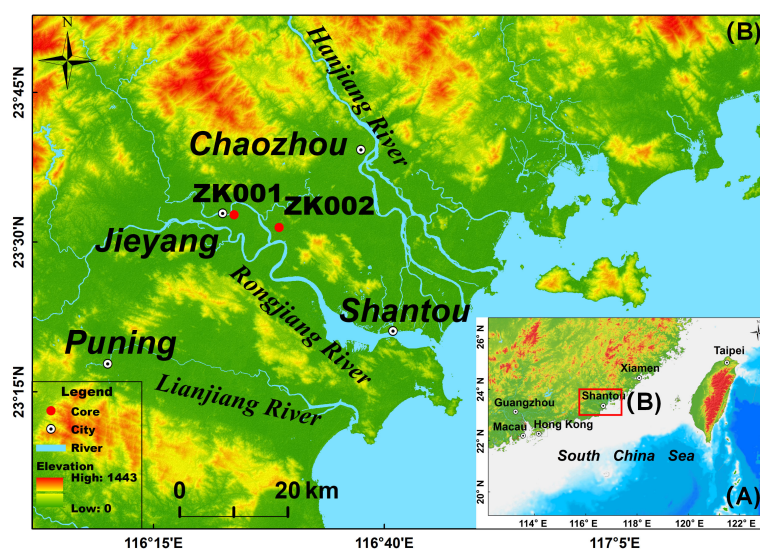


FIGURE 1

Location of the Chaoshan plain and sites of cores ZK001 and ZK002. (A) General map around the Chaoshan plain; red square box encompasses the major area of the Chaoshan plain. (B) The major area of the Chaoshan plain consists of the Hanjiang Delta, the Rongjiang alluvial plain, and the Lianjiang alluvial plain; two boreholes including cores ZK001 and ZK002 were obtained from the Rongjiang alluvial plain. Base maps are from <http://www.gscloud.cn/> and <https://www.ngdc.noaa.gov/mgg/global/global.html>.

Geological setting and samples

The Chaoshan plain is located on the southeastern coast of China and borders the South China Sea. It consists of the Hanjiang Delta, the Rongjiang alluvial plain, and the Lianjiang alluvial plain and covers an area of 2,600 km² (Figure 1) (Li et al., 1987; Wang et al., 1997). The plain was developed during the Mesozoic Yanshan epoch and is mainly dissected by NE and NW direction fault zones (Li et al., 1987; Liu, 1995). Different uplift and subsidence movements during the Neogene to the early Quaternary transformed the Chaoshan plain into a down-faulted basin (Wang et al., 1997). This resulted in the creation of large accommodation spaces, with an average depth of up to 76.5 m, for the deposition of Quaternary sediments (Wang et al., 1997). The highest thickness of sedimentary sequences has been found in the Hanjiang Delta, the Rongjiang plain, and the Lianjiang plain at 168 m, 90 m, and 141.2 m, respectively (Chen, 1984a; Liu, 1995; Zhou, 2008).

Two terrestrial cores (ZK001 and ZK002) were obtained from Jieyang, the northwestern part of the Rongjiang plain by rotary drilling. Core ZK001 is located in Rongcheng District (116°23'36" E, 23°32'51" N; 8 m above sea level (asl)), with a depth of 90.85 m. Core ZK002 lies in Paotai Town (116°28'30"E, 23°31'36"N; 2 m asl), with a depth of 100 m. Both cores ZK001 and ZK002 are dominated by dark gray clay, gray silty clay, and yellowish or grayish-white coarse sands with gravel (Figure 4). Seven OSL samples dating samples were collected from core ZK001 and six from core ZK002. Four plant remains were obtained for ¹⁴C dating from core ZK001, and eleven plant remains and three rotten leaves from core ZK002.

Methods

Radiocarbon dating

Eighteen samples from cores ZK001 and ZK002 were treated and analyzed at the accelerator mass spectrometry (AMS) laboratory of Peking University for ¹⁴C dating. The half-life of ¹⁴C used for age calculation in this study was Libby's half-life (5,568 ± 30 a). The ¹⁴C ages were calibrated to calendar years (cal a BP or cal ka BP) using IntCal20 atmospheric calibration curves (Reimer et al., 2020) using the OxCal v4.4.4 program with a 95.4% calibrated range (Ramsey and Lee, 2013). The calibrated ¹⁴C ages were converted to ka for comparison with OSL ages.

OSL dating

A total of thirteen samples from cores ZK001 and ZK002 were collected for OSL dating. The laboratory work, including sample preparation and measurement, was carried out under

subdued red light according to the luminescence dating procedures (Lai and Wintle, 2006; Lai, 2010). The light-exposed outer samples were used to measure dose rate and water content, while the remaining samples were treated sequentially with 10% HCl and 30% H₂O₂ to remove carbonates and organic materials. Wet sieving was used to obtain 38 - 63 μm and 90 - 125 μm fractions based on fraction availability in the sediments. Mid-grained fractions (38–63 μm) were etched by 35% H₂SiF₆ for 2 weeks, while coarse-grained fractions (90–125 μm) were treated with 40% HF for ~30 min to obtain pure quartz and then washed with 10% HCl for about 30 min to remove acid-soluble fluoride. The purity of quartz was checked by infrared-stimulated luminescence (IRSL) signals. Mid-grained fractions (38–63 μm) were pretreated with H₂SiF₆ again because of obvious IRSL signals (beyond 10%) (Lai and Brueckner, 2008). However, the IRSL results still show obvious signals even after retreatment with H₂SiF₆ twice. Therefore, quartz signals of all treated mid-grains (38–63 μm) were stimulated by involving post-IR OSL signal (Roberts and Wintle, 2003). The treated grains were then mounted on the center (7 mm diameter) of 9.7-mm-diameter stainless-steel discs using silicone oil for D_e measurements.

OSL measurements were conducted on a Risø TL/OSL-DA-20 reader equipped with a ⁹⁰Sr/⁹⁰Y beta source and blue LEDs (λ = 470 ± 20 nm) (Bøtter-Jensen et al., 1999). All optical stimulation (IR and blue-light) measurements for mid-grains (38–63 μm) and coarse-grained quartz (90–125 μm) were stimulated at 130°C for 40 s and recorded by an EMI 9235QA photomultiplier tube fitted with a 7.5-mm Hoya U-340 filter. The equivalent dose (D_e) in this study was measured by the SAR-SGC method (Lai and Ou, 2013), a combination of the single-aliquot regenerative dose (SAR) protocol (Murray and Wintle, 2000) and standard growth curve (SGC) (Roberts and Duller, 2004; Lai, 2006; Lai et al., 2007). The preheat temperature for natural and regenerative dose signals was 260°C for 10 s, and the preheating temperature for test dose response was 220°C for 10 s (Wintle and Murray, 2006). For each sample, 5–6 aliquots were measured by SAR protocol to establish an SGC curve, and 6–12 aliquots were measured by SGC protocol. The final D_e value for a sample age calculation was the average of all D_e values measured by both SAR and SGC protocols.

Inductively coupled plasma mass spectrometry (ICP-MS) was used to measure uranium (U), and thorium (Th), and inductively coupled plasma/optical emission spectrometry (ICP/OES) was used to determine potassium (K). The cosmic ray dose was calculated depending on the depth, altitude, and geomagnetic latitude of each sample (Prescott and Hutton, 1994). The shielding effect of water must be considered when calculating the water content because a 1% increase/decrease in the average water content during the lifetime will usually lead to a 1% increase/decrease in the dose rate (Wallinga and Cunningham, 2015; Murray et al., 2021). Variations in water

content over geologic time can have a significant effect on the dose rate in sediments, and uncertainties in dose rate are large because of the poorly understood history of water content (Lai and Ou, 2013; Wallinga and Cunningham, 2015). The measured water content for cores ZK001 and ZK002 range between 7.4% and 40.5% and between 8% and 18.2%, respectively. Yet, the measured water content cannot accurately reflect the real water content of the sediments at the time of burial. Therefore, based on the variation of water content within the burial period in the study region, we estimated the water content to be $25\% \pm 5\%$ for all OSL samples in this study instead of using the measured water content.

Results

Radiocarbon ages

^{14}C results of cores ZK001 and ZK002 are listed in Table 1 and can be shown in Figure 4. The plant remains ages of core ZK001 are infinite (>40 ka BP) because these ages are out of the calibration range. The age of the rotten leaves obtained from sample ZK002-C14-01 (3.8 m depth) at 19.34 ± 0.17 cal ka BP is considered overestimated. Plant remains from sample ZK002-C14-04 (18.05 m depth) are dated to 8.81 ± 0.17 cal ka BP, and rotten leaves from sample ZK002-C14-05 (18.95 m depth) are dated to 9.15 ± 0.13 cal ka BP; both are consistent with the stratigraphic order. At depths below 31 m, one sample of rotten leaves and three plant remains have ^{14}C ages that are infinite (>40 ka BP), and the other seven plant

remains have finite ages showing age reversals. Potential reasons for age reversals will be discussed below.

OSL ages

OSL ages are listed in Table 2 and can be shown in Figure 4. In core ZK001, the age range is from 1.7 ± 0.1 ka to 56 ± 4.8 ka, and in core ZK002, the age range is from 15 ± 1.1 ka to 177 ± 20 ka. OSL ages of eight samples, namely, ZK001-G12, ZK001-G13, ZK001-G14, ZK002-G02, ZK002-G03, ZK002-G04, ZK002-G05, and ZK002-G06, are considered as minimum ages because of the OSL signal saturation (D_e exceeds 150 Gy) (Wintle and Murray, 2006; Murray et al., 2021). In general, OSL ages of cores ZK001 and ZK002 are in stratigraphic order. Recycling ratio and recuperation are key factors for evaluating the SAR protocol for D_e determination (Wintle and Murray, 2006). The accepted D_e aliquots for each sample in this study matched the criteria of recycling ratios between 0.9 and 1.1 and recuperation ratios of $<5\%$. Representative OSL decay and growth curves of samples ZK001-G04 and ZK002-G01 are shown in Figure 2. The decay curves show that the OSL intensity decreased rapidly to background levels within 2 s, indicating the dominance of the fast components (Wintle and Murray, 2006). The representative growth curves of samples ZK001-G04 and ZK002-G01 are well-fitted, indicating the applicability of a combined SAR-SGC method in this study (Figure 2). Furthermore, the D_e determined by the SGC is consistent with the D_e determined by the SAR protocol.

TABLE 1 ^{14}C ages for samples from cores ZK001 and ZK002, the Chaoshan plain.

Sample ID	Depth (m)	Dating material	^{14}C age (a BP)	Calibrated age (95.4% calibrated range, cal ka BP)
ZK001-C14-10	37.62	Plant remains	$>40,820$	–
ZK001-C14-11	41.46	Plant remains	$>40,820$	–
ZK001-C14-13	54.80	Plant remains	$>40,820$	–
ZK001-C14-14	56.58	Plant remains	$>40,820$	–
ZK002-C14-01	3.8	Rotten leaves	$16,030 \pm 60$	19.34 ± 0.17
ZK002-C14-04	18.05	Plant remains	$7,935 \pm 35$	8.81 ± 0.17
ZK002-C14-05	18.95	Rotten leaves	$8,195 \pm 30$	9.15 ± 0.13
ZK002-C14-06	30.95	Plant remains	$>40,820$	–
ZK002-C14-07	33.3	Plant remains	$>40,820$	–
ZK002-C14-08	40	Rotten leaves	$>40,820$	–
ZK002-C14-10	57.76	Plant remains	$35,450 \pm 220$	40.57 ± 0.51
ZK002-C14-11	59.32	Plant remains	$34,130 \pm 240$	39.22 ± 0.66
ZK002-C14-12	64.81	Plant remains	$>40,820$	–
ZK002-C14-14	74.54	Plant remains	$28,970 \pm 230$	33.27 ± 0.92
ZK002-C14-15	87.15	Plant remains	$36,440 \pm 250$	41.47 ± 0.42
ZK002-C14-16	91.6	Plant remains	$30,900 \pm 190$	35.21 ± 0.51
ZK002-C14-17	94.16	Plant remains	$30,980 \pm 170$	35.31 ± 0.52
ZK002-C14-18	96.43	Plant remains	$32,850 \pm 240$	37.43 ± 0.90

TABLE 2 OSL dating results for samples from cores ZK001 and ZK002, the Chaoshan plain.

Sample ID	Depth (m)	Dating material	Grain size (μm)	Aliquot number	U (ppm)	Th (ppm)	K (%)	Water content (%)	Dose rate (Gy/ka)	D _e (Gy)	OSL age (ka)
ZK001-G01	0.9	Polymineral	38–63	6 ^a + 11 ^b	4.9 ± 0.24	28.1 ± 2.81	2.44 ± 0.29	25 ± 5	5.11 ± 0.29	8.7 ± 0.4	1.7 ± 0.1
ZK001-G03	8.9	Polymineral	38–63	6 ^a + 10 ^b	4.77 ± 0.24	24 ± 2.4	2.24 ± 0.27	25 ± 5	4.81 ± 0.27	17.2 ± 0.5	3.6 ± 0.2
ZK001-G04	10.5	Polymineral	38–63	5 ^a + 12 ^b	4.36 ± 0.22	22.4 ± 2.24	1.96 ± 0.24	25 ± 5	4.59 ± 0.26	23.8 ± 0.4	5.2 ± 0.3
ZK001-G08	14.5	Polymineral	38–63	5 ^a + 12 ^b	8.02 ± 0.4	27.63 ± 2.76	4.28 ± 0.51	25 ± 5	5.94 ± 0.33	135 ± 1.7	23 ± 1.3
ZK001-G12	21.2	Quartz	90–125	4 ^a + 10 ^b	11.1 ± 0.55	33.76 ± 3.38	2.87 ± 0.34	25 ± 5	6.09 ± 0.33	>231 ± 18 ^c	>38 ± 3.7 ^d
ZK001-G13	21.5	Quartz	90–125	5 ^a + 12 ^b	5.78 ± 0.29	23.64 ± 2.36	2.33 ± 0.28	25 ± 5	4.16 ± 0.24	>235 ± 14 ^c	>56 ± 4.8 ^d
ZK001-G14	23.4	Polymineral	38–63	12 ^b	3.22 ± 0.16	10.23 ± 1.02	2.89 ± 0.35	25 ± 5	3.86 ± 0.22	>211 ± 4.2 ^c	>55 ± 3.3 ^d
ZK002-G01	19.9	Quartz	90–125	6 ^a + 12 ^b	2.03 ± 0.1	9.58 ± 0.96	0.66 ± 0.08	25 ± 5	1.43 ± 0.08	22 ± 0.9	15 ± 1.1
ZK002-G02	26.5	Quartz	90–125	5 ^a + 12 ^b	10.14 ± 0.51	28.97 ± 2.9	2.84 ± 0.34	25 ± 5	5.63 ± 0.31	>153 ± 7.3 ^c	>27 ± 2.0 ^d
ZK002-G03	41.1	Quartz	90–125	4 ^a + 12 ^b	5.53 ± 0.28	30.73 ± 3.07	1.43 ± 0.17	25 ± 5	3.78 ± 0.21	>204 ± 7.9 ^c	>54 ± 3.6 ^d
ZK002-G04	49.8	Quartz	90–125	11 ^b	1.28 ± 0.06	4.86 ± 0.49	1.11 ± 0.13	25 ± 5	1.37 ± 0.1	>191 ± 10 ^c	>140 ± 12 ^d
ZK002-G05	83.6	Quartz	90–125	10 ^b	5.74 ± 0.29	8.29 ± 0.83	1.4 ± 0.17	25 ± 5	2.58 ± 0.15	>280 ± 15 ^c	>109 ± 8.5 ^d
ZK002-G06	93	Quartz	90–125	10 ^b	2.88 ± 0.14	5.16 ± 0.52	0.28 ± 0.03	25 ± 5	1.02 ± 0.05	>180 ± 18 ^c	>177 ± 20 ^d

^aNumbers of aliquots measured using the standard SAR method.

^bNumbers of aliquots measured using the standard SGC method. ^cMinimum D_e. ^dMinimum age.

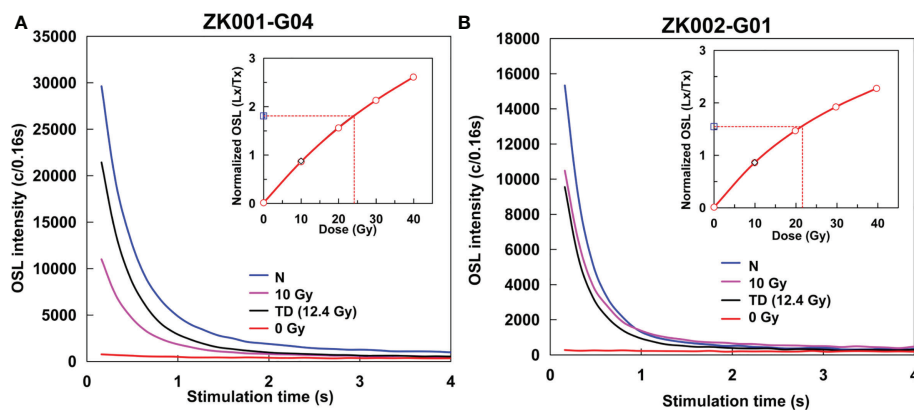


FIGURE 2

OSL decay and growth curves of samples ZK001-G04 (A) and ZK002-G01 (B). The growth curves show the dose–response L_x/T_x (where L_x is the ratio of the luminescence signal and T_x is the fixed dose). The decay curves of the natural dose (N), regeneration dose (R), and test dose (TD = 12.4 Gy) show the OSL signals decreasing rapidly during the first second of stimulation, indicating that the OSL signal is dominated by the fast component in these samples.

Discussion

Reliability and upper limit of plant remains ^{14}C dating by comparison with quartz OSL dating Cores

ZK001 and ZK002 were used to reconstruct paleoenvironmental changes by combining the Holocene diatom records, chronology, and sedimentology analysis (Zhang et al., 2020). In addition, the basal Quaternary deposits from core ZK002 were used to establish a new lithostratigraphic unit named the Paotai Formation in the Chaoshan plain (Ling et al., 2021). While the main objectives of this study are to explore the practical detection limit of ^{14}C dating using plant remains and to determine the age of onset of Quaternary deposition in the area.

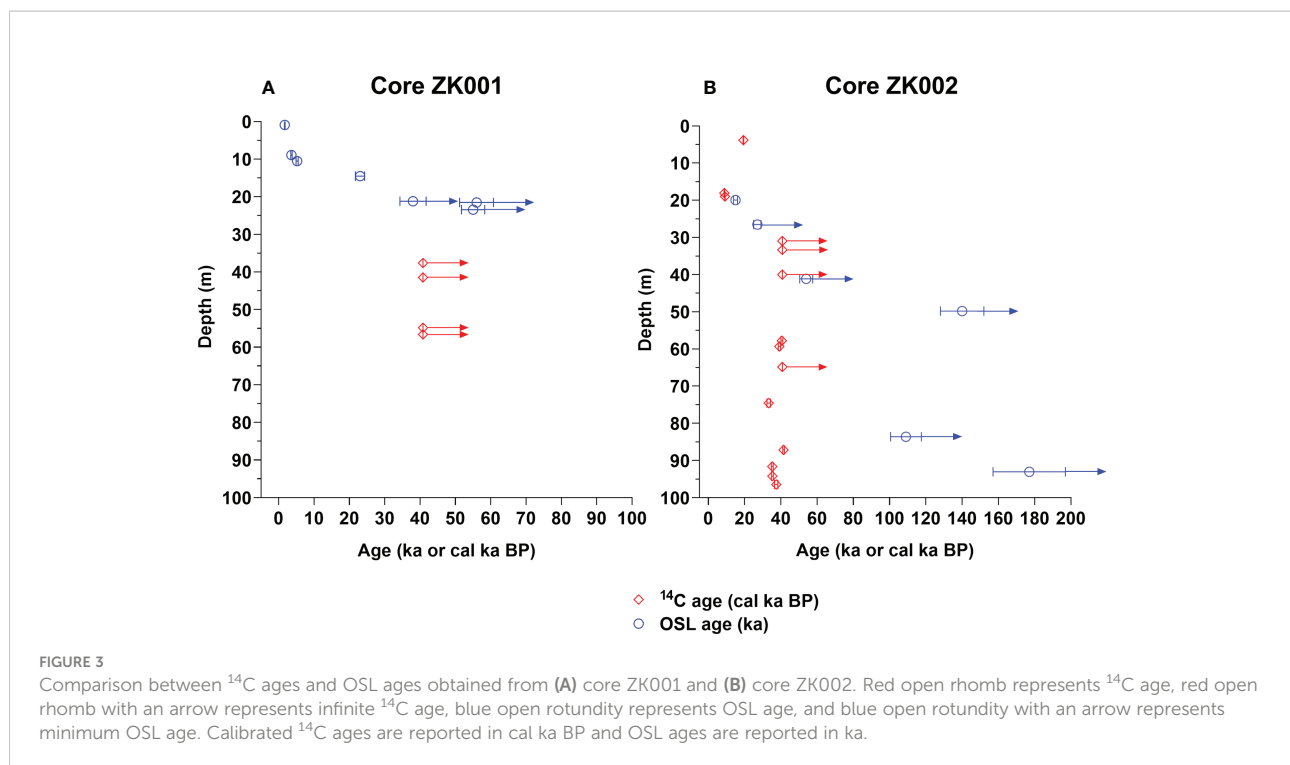
Eighteen ^{14}C samples of plant remains and rotten leaves from the Rongjiang alluvial plain were dated in this study to obtain a detailed chronological framework. The results show that eight samples are infinite (>40.82 ka BP) and others show age reversals. One rotten leaves ^{14}C age (ZK002-C14-01; 19.34 ± 0.17 cal ka BP) was collected from core ZK002 at a depth of 3.8 m. Plant remains ^{14}C age (ZK002-C14-04; 8.81 ± 0.17 cal ka BP) at a depth of 18.05 m and rotten leaves ^{14}C age (ZK002-C14-05; 9.15 ± 0.13 cal ka BP) at a depth of 18.95 m from a peat layer are consistent with stratigraphic order. Compared with the dates below, rotten leaves ^{14}C age at the top (ZK002-C14-01) is reversed. Potential reasons for age reversals could be (1) sedimentary environment disturbances, (2) the erosion and re-deposition of older sediments, and (3) reworking along the dispersal path from the catchment area to the coast (Goodfriend and Stipp, 1983; Stanley and Chen, 2000; Nian et al., 2018). The layer at the top (3.8 m in depth) of core ZK002 is characterized by a tidal flat phase composed of dark gray silt and silty clay with insets of rotten wood, plants, and shell fragments. Disturbances in the sedimentary environment of the tidal flats might be the ultimate cause of age reversal at the top of the core.

^{14}C age reversals are also common in core ZK002 at depths below 31 m. All reversed ^{14}C ages are significantly underestimated and are not in agreement with quartz OSL ages. Quartz OSL ages of core ZK002 are stratigraphically consistent with general depths, ranging from 15 ka to 177 ka. The comparison between ^{14}C and OSL ages from cores ZK001 and ZK002 is shown in Figure 3. OSL and ^{14}C from core ZK002 at depths greater than ca. 30 m yielded consistent ages up to ca. 35 cal ka BP, while the difference becomes greater beyond 35 cal ka BP. All ^{14}C ages of core ZK002 below ca. 30 m depth are not in agreement with stratigraphic order and clustered around 35–41 cal ka BP. However, OSL ages of core ZK002 successively increase at depths below ca. 30 m, with ages ranging from 54 ka to 177 ka (Figure 4; Table 2). In particular, three ^{14}C ages of plant remains (35–37 cal ka BP) below ca. 91 m depth were underestimated compared with quartz OSL age (ZK002-G06, $>177 \pm 20$ ka).

The potential reasons for the discrepancy between ^{14}C and OSL ages in this study need to be investigated. Because of groundwater-level fluctuations and wet–dry seasonal variations in hydrochemistry in coastal plains and swamps, contamination of humus could occur at different times (Zhang and Shi, 1989). In addition, microbial or plant activities can lead to contamination. For instance, when the organisms (e.g., photosynthetic algae) in sediments are exposed to the atmosphere, they metabolize and produce new organic matters. This process can introduce modern carbon into the sediments, leading to an underestimation of the true age (Cheng et al., 2020). Plant activity such as tree roots could also alter the organic composition of sediments, which could be identified as secondary organic material prior to ^{14}C dating (Palstra et al., 2021). Modern carbon contamination in peat and carbonaceous material cannot be completely eliminated even if some effective pretreatment techniques are used [e.g., acid–base–acid (ABA) and acid–base oxidation (ABOX) pretreatment]. Consequently, the dated samples represent a mixture of old and young carbon that cannot yet be separated at the present time (Bird et al., 1999; Hatté et al., 2001; Agatova et al., 2019).

The amount of original ^{14}C used for age determination in an old sample is scarce due to the half-life ($5,730 \pm 40$ a) of ^{14}C , implying that it is susceptible to modern carbon contamination. The effect of contamination increases with age; even a small amount of secondary carbon can lead to significant errors (Pigati et al., 2007). Sediments at depths of ca. 91–97 m in core ZK002 are terrestrial swamp facies, composed of dark gray silt and clay with fine sands. Contaminant carbon such as humus probably causes an underestimation of the ^{14}C ages of plant remains underestimation at a depth of ca. 91–96 m in terrestrial swamp facies. Finite ^{14}C ages within these layers do not determine depositional dates because they may be intrusive or residual from bioturbation and post-depositional processes. Zheng and Li (2000) have also suggested that radiocarbon dates from terrestrial weathered samples in the Chaoshan plain may have been contaminated by young carbon during periods of low sea level. Contamination with modern carbon is probably the main factor that resulted in the underestimation of the ^{14}C age in this study.

The significant age discrepancy between ^{14}C and OSL from the Chaoshan plain is not particular. Several studies demonstrated that the radiocarbon ages are inconsistent with OSL ages for pre-Holocene samples (Liu and Lai, 2012; Sun et al., 2012; Zhao et al., 2013; Madsen et al., 2014). Regardless of the materials, ^{14}C ages are much younger than luminescence ages. Inconsistencies between ^{14}C and OSL dating have been reported in arid regions in China. Lai et al. (2014) compared previous ^{14}C ages with new OSL ages on lacustrine sediments from Qaidam Basin, northeastern Qinghai-Tibetan Plateau (QTP), and found that the radiocarbon ages of 25–40 ka BP (MIS3) are older by up to approximately 100 ka (MIS 5) using OSL. They suggested that ^{14}C ages older than approximately 25 ka BP are severely



underestimated, especially for samples from arid regions. The following study from the Ili Basin in Central Asia has confirmed that ^{14}C ages older than 25 cal ka BP are greatly underestimated in other terrestrial deposits in Central Asia (Song et al., 2015). Song et al. (2015) concluded that the ^{14}C ages of >30 cal ka BP from the Ili Basin are scattered between the 2% and 3%–4% modern carbon contamination lines. The problem of underestimation of radiocarbon ages also exists in humid regions. The contrast between ^{14}C ages using plant remains and quartz OSL ages is reported from the Dongjiang plain, southwest of the Chaoshan plain, with an age difference of more than 30 ka when dating sediments beyond ca. 33 ka BP (Guo et al., 2013). Similarly, using plant macrofossil to date Devensian fluvial sediments in lowland Britain, Briant and Bateman (2009) found that radiocarbon ages beyond 40 cal ka BP were remarkably younger than OSL ages. All conventionally pretreated ABA radiocarbon ages fall in the range of ca. 40–45 cal ka BP, while OSL dates fall between ca. 69 and 110 ka (Briant and Bateman, 2009). Likewise, results from Weichselian alluvial in the Netherlands also showed that all ^{14}C ages of Eerbeek-I below 2 m depth were infinite ages (>45.4 cal ka BP), while the OSL dates fall in ca. 49–102 ka at the same depth (Palstra et al., 2021).

It is suggested that plant remains are the ideal material for ^{14}C dating (Nilsson et al., 2001; Reimer, 2012; Väiliranta et al., 2014), but ^{14}C ages in this study along with research from fluvial sediments (lowland Britain) (Briant and Bateman, 2009) and Weichselian alluvial (the Netherlands) (Palstra et al., 2021)

demonstrated that it is challenging for ^{14}C dating when samples are >35 cal ka BP in practice. Extreme caution is needed to interpret the reliability of published ^{14}C ages beyond 40 ka BP. It is necessary to select plant materials that were most likely part of the original deposit (such as leaves or seeds) when feasible (Briant and Bateman, 2009). The influence of different geological environments on the ^{14}C dating source material should be considered when using ^{14}C ages to establish an age model (Zhang and Shi, 1989; Cheng et al., 2022). Combining radiocarbon dating with different dating techniques is suggested to obtain reliable results.

Luminescence dating has proven useful in addressing the upper age limit (beyond 35 cal ka BP) of radiocarbon dating. Quartz OSL has the advantages of rapid bleaching and signal stability. However, quartz encounters a problem of underestimating the true age at larger doses (150–250 Gy) (Lai, 2006; Wintle and Murray, 2006; Lai, 2010; Lai and Fan, 2014; Ou et al., 2014; Wang et al., 2018b; Li et al., 2020a; Li et al., 2020b; Murray et al., 2021; Xu et al., 2021). Underestimation of quartz OSL age due to saturation was found in estuarine and marine regions. D_e values of quartz OSL samples > 200 Gy from borehole TJC-1 in the western Bohai Sea, China, showed saturated ages beyond 80 ka (Long et al., 2022). Quartz OSL samples from core HPQK01 in Pearl River Delta have also shown that quartz OSL ages ranging from 125 ± 18 ka to 58 ± 6 ka are considered minimum ages due to the OSL saturation >150 Gy (Xu et al., 2022). D_e results (Table 2) show that seven quartz OSL and one polymineral sample have D_e s up to 150 Gy,

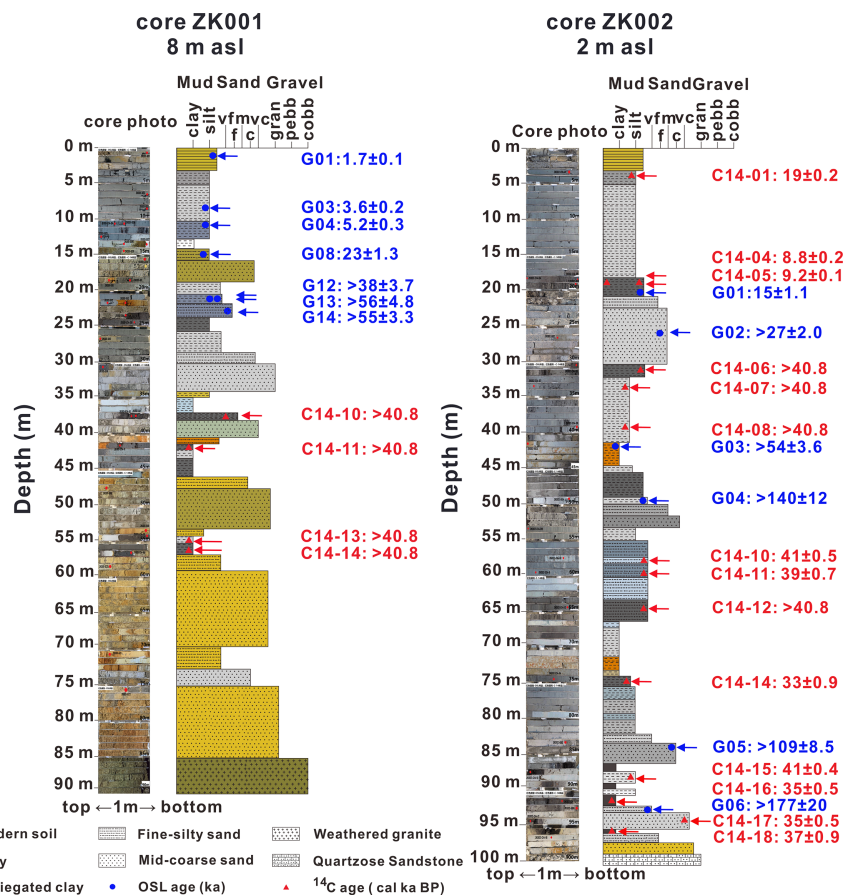


FIGURE 4 Profiles and ages of cores ZK001and ZK002. The red triangle represents the ¹⁴C age; blue circle represents the OSL age.

including ZK001-G12 (>231 Gy, 21.2 m in depth), ZK001-G13 (>235 Gy, 21.5 m in depth), ZK001-G14 (>211Gy, 23.4 m in depth), ZK002-G02 (>153 Gy, 26.5 m in depth), ZK002-G03 (>204 Gy, 41.1 m in depth), ZK002-G04 (>191 Gy, 49.8 m in depth), ZK002-G05 (>280 Gy, 83.6 m in depth), and ZK002-G06 (>180 Gy, 93 m in depth). Usually, OSL growth curves can be fitted with a single saturating exponential function of the form $I(D)/I_s = (1 - \exp(-D/D_0))$, where I is the OSL signal intensity, I_s is the saturation intensity, D is the absorbed radiation dose, and D_0 is indicative of the onset of saturation (Singarayer and Bailey, 2003; Wintle and Murray, 2006; Wallinga and Cunningham, 2015). Wintle and Murray (2006) suggested that the reliable D_e should be less than $2 * D_0$ when the OSL signal is about 15% below the saturation level based on the assumption of exponential growth. A representative growth curve of five aliquots up to 280 Gy for sample ZK002-G02 (Figure 5) was constructed to investigate the degree of saturation. When fitting a single exponential [$Y = 9.62 * (1 - \exp(-X/156.1))$] (Figure 5), the maximum reliable D_e of sample ZK002-G02 is 312 Gy

($2 * D_0$). The values of D_0 and $2 * D_0$ for eight saturated samples are given in Table 3. The D_e values of samples ZK001-G12, ZK001-G13, and ZK001-G14 are greater than $2 * D_0$ (Tables 2 and 3), indicating OSL saturation. As discussed previously, the saturation dose of estuarine samples is approximately 150–200 Gy (Long et al., 2022; Xu et al., 2022). Therefore, the D_e s of five samples from core ZK002 are more likely to reach the saturation level, even if these values are lower than $2 * D_0$ (Tables 2, 3). The obtained ages of these samples should be considered as minimum ages for paleoenvironmental reconstruction.

Late Quaternary chronological framework of cores ZK001 and ZK002 based on ¹⁴C and OSL dating

The chronology of Quaternary deposits in the Chaoshan plain is lacking reliability since most previous work has relied essentially on a radiocarbon dating method confined to ca. 40 ka

TABLE 3 Values of D_0 and 2^*D_0 for samples from core ZK001 and ZK002.

Sample ID	D_0 (Gy)	2^*D_0 (Gy)
ZK001-G12	101	202
ZK001-G13	116	232
ZK001-G14	116	232
ZK002-G02	156	312
ZK002-G03	183	366
ZK002-G04	183	367
ZK002-G05	185	369
ZK002-G06	181	363

* represents a multiplication sign.

BP (Li et al., 1987; Li et al., 1988). Fossils of rhinoceros, giant pandas, and saber-toothed elephants from an alluvial layer in Jieyang County show that the deposition of the Quaternary sediments in the Chaoshan plain began as early as the middle Pleistocene (Chen, 1984b). On the contrary, some studies argue that the basal part of the Quaternary sediments (fluvial sediments, named the Nanshe Formation) in the Chaoshan plain was deposited no more than 55 ka BP based on ^{14}C , TL ages, and stratigraphic relationships (Chen, 1984a; Li et al., 1987; Li et al., 1988). According to the chronologies published so far, the Nanshe Formation is overlain by a lower marine unit (M2, also named the Jiali Formation) dated at MIS 3 based on ^{14}C (Li et al., 1987; Li et al., 1988). Zong et al. (2015) suggested that the global sea level during MIS 5e (ca. 130–120 ka) (Rohling et al.,

2008) was possibly 3–5 m higher than the present sea level but dropped to 60–80 m below the present sea level (BSL) during MIS 3 (ca. 58–24 ka) (Bard et al., 1990; Yokoyama et al., 2001). The depositional surface was very close to the present sea level during the deposition of the lower marine sequence in the Chaoshan plain, as the sea level during MIS 5e was several meters higher than the present (Zong et al., 2015). Accordingly, Zong et al. (2015) demonstrated that the lower marine unit (M2) was deposited at a depth of around 45 to 80 m BSL; therefore, the actual age is likely to be older than MIS 5, rather than MIS 3. Subsequent studies from the Lianjiang plain, the southeastern part of the Chaoshan plain, have confirmed these findings using ESR and OSL (Song et al., 2012; Tang et al., 2018). The combination of ^{14}C , OSL, and ESR dating, of the lower marine unit (M2) from the Lianjiang plain, shows that the results are also at MIS 5 rather than MIS 3 (Song et al., 2012; Tang et al., 2018). ESR ages of the basal terrestrial layer from the core WYZK-06 (at a depth of ca.100–130 m) in the Lianjiang plain fall approximately within MIS 7 (ca. 243–190 ka) to MIS 6 (ca. 190–130 ka) (Song et al., 2012). Quartz OSL dates (>216 ka) from core CN-01 (23.57 m depth) in the Lianjiang plain also indicate that the basal terrestrial sediments were deposited mainly during a substage of MIS7 (Tang et al., 2018). In this study, the oldest quartz OSL age from core ZK002 in the Rongjiang plain (middle part of the Chaoshan plain) is $>177 \pm 20$ ka (ZK002-G06, 93 m depth), which is much older than the results of previous studies (Chen, 1984a; Li et al., 1987; Li et al., 1988). The onset of deposition (consisting of coarse sand with

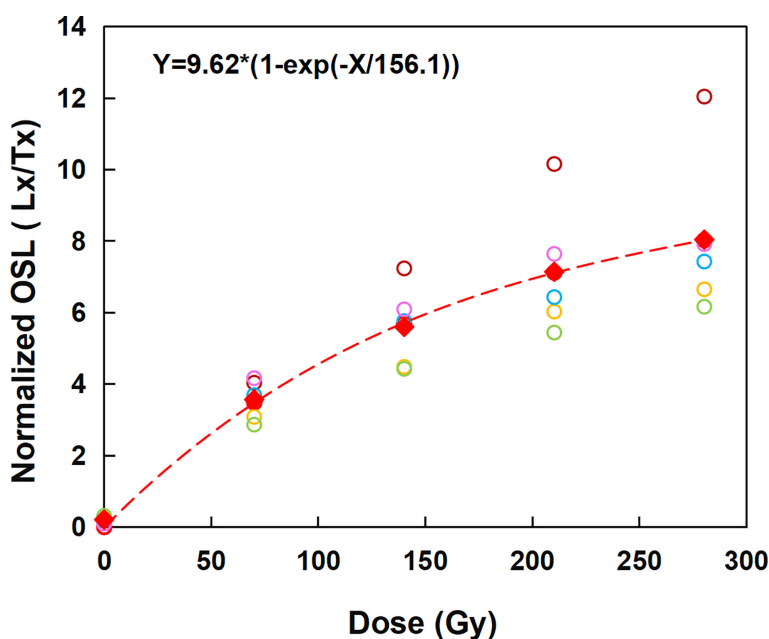


FIGURE 5 Growth curves of five aliquots up to 280 Gy for sample ZK002-G02. The dotted line denotes the average growth curve of the five aliquots.

gray-white color) in the Rongjiang plain is probably attributed to MIS 6 during the sea level lowstand, which was mainly influenced by fluvial processes.

The variegated clay is a weathered clay of fluvial deposits formed in a low-stand fluvial environment and is considered an important cycle boundary with hiatus in the coastal areas of the South China Sea. The results from the Pearl River Delta show that the first and second variegated clay layers were formed during the last glacial maximum (LGM) (ca. 30–20 ka) and MIS 4 (ca. 74–60 ka), respectively (Xie et al., 2014). Variegated clay layers are also found in this study in cores ZK001 and ZK002. The hiatus (from ca. 23 ± 1.3 ka to 5.2 ± 0.3 ka) of core ZK001 occurred at a depth of ca. 10.5–14.5 m, with sediments composed of clay and variegated clay. Quartz OSL age (ZK001-G08, 23 ± 1.3 ka, 14.5 m depth) confirmed that variegated clay in this layer was deposited during the LGM in a low-stand fluvial environment (Figure 4). Hiatus (from ca. 15 ka to 9.2 cal ka BP) was also observed in core ZK002 at ca. 19–20 m depth (Figure 4). The sediments in this layer are composed of fluvial sediments of gray-white fine sands without variegated clay deposited mainly during the LGM. Unlike core ZK001, two variegated clay layers are recorded in core ZK002. The first variegated clay layer (ca. 41–45 m in depth) was likely to be deposited during MIS 4 based on the quartz OSL age (ZK002-G03, $>54 \pm 3.6$ ka) at a depth of 41.1 m. The second variegated clay layer (ca. 69–74 m in depth) has not been dated in this study due to suitable sample insufficiency. However, we speculate that this layer is likely deposited by a fluvial channel in a sea-level lowstand environment. An obvious lithologic change from fine-grained clay with gray-white color at the bottom to silt with deep gray color on the top can be seen across the hiatus in core ZK001 at a depth of ca. 11–15 m. This variation in lithology is also recorded around the hiatus in core ZK002, from coarse sand with gravel in steel gray color at the bottom to middle-fine grain sand with gray color within a depth of ca. 19–30 m across the hiatus. The change in lithology around the depositional hiatus in both cores ZK001 and ZK002 reflects a change in the paleoenvironment from a fluvial to a coastal environment in response to sea-level change.

Conclusions

In this study, we applied ^{14}C and OSL methods to date the late Quaternary sediments from two cores, ZK001 and ZK002, from the Rongjiang plain. Chronological data based on ^{14}C and OSL dating methods from both cores show discrepancies in dates older than 35 cal ka BP. ^{14}C ages were significantly younger than their corresponding OSL ages, suggesting that ^{14}C dating is underestimated. Instead, OSL dating is well applicable to provide a reliable chronology older than 35 ka. In addition, the oldest OSL age (ZK002-G06, $>177 \pm 20$ ka, 93 m depth) from core

ZK002 indicates that the onset of sediment accumulation in the Rongjiang plain could be traced back to at least MIS 6.

Data availability statement

The original contributions presented in the study are included in the article/supplementary material. Further inquiries can be directed to the corresponding author.

Author contributions

JZ: Data curation, Visualization, Writing-Original draft. LK: Data curation, Investigation. MY: Data curation, Investigation. QS: Data curation, Investigation. MA: Writing- Reviewing and Editing. ZL: Conceptualization, Methodology, Supervision, Funding acquisition, Reviewing and Editing. All authors contributed to the article and approved the submitted version.

Funding

This research was supported by the China Geological Survey Project (Grants No. DD20160032-14), National Natural Science Foundation of China (Grants No. 41877438), STU Scientific Research Start-Up Foundation for Talents (NTF19003, NTF20006), and Innovation and Entrepreneurship Project of Shantou (2021112176541391).

Acknowledgments

We thank Xianmei Huang for the helpful discussions and Junxiang Miao for sample collection

Conflict of interest

The authors declare that the research was conducted in the absence of any commercial or financial relationships that could be construed as a potential conflict of interest.

Publisher's note

All claims expressed in this article are solely those of the authors and do not necessarily represent those of their affiliated organizations, or those of the publisher, the editors and the reviewers. Any product that may be evaluated in this article, or claim that may be made by its manufacturer, is not guaranteed or endorsed by the publisher.

References

- Agatova, A. R., Nepop, R. K., Bronnikova, M. A., Zhdanova, A. N., Moska, P., Zazovskaya, E. P., et al. (2020). Problems of ^{14}C dating in fossil soils within tectonically active highlands of Russian Altai in the chronological context of the late pleistocene megafloods. *Catena* 195, 104764. doi: 10.1016/j.catena.2020.104764
- Agatova, A., Nepop, R., Zazovskaya, E., Ovchinnikov, I., and Moska, P. (2019). Problems of developing the pleistocene radiocarbon chronology within high mountain terraces by the example of Russian Altai. *Radiocarbon* 61 (6), 2019–2028. doi: 10.1017/RDC.2019.83
- Al-Saqarat, B. S., Abbas, M., Lai, Z., Gong, S., Alkuisi, M. M., Hamad, A. M. A., et al. (2021). A wetland oasis at wadi gharandal spanning 125–70 ka on the human migration trail in southern Jordan. *Quaternary Res.* 100, 154–169. doi: 10.1017/qua.2020.82
- Bøtter-Jensen, L., Duller, G., Murray, A., and Banerjee, D. (1999). Blue light emitting diodes for optical stimulation of quartz in retrospective dosimetry and dating. *Radiat. Prot. Dosimetry* 84 (1–4), 335–340. doi: 10.1093/oxfordjournals.rpd.a032750
- Bard, E., Hamelin, B., and Fairbanks, R. G. (1990). U-Th Ages obtained by mass spectrometry in corals from Barbados: sea level during the past 130,000 years. *Nature* 346 (6283), 456–458. doi: 10.1038/346456a0
- Bird, M. I., Ayliffe, L. K., Fifield, L., Turney, C. S. M., Cresswell, R. G., Barrows, T. T., et al. (1999). Radiocarbon dating of “old” charcoal using wet oxidation stepped-combustion procedure. *Radiocarbon* 41 (2), 127–140. doi: 10.1017/S0033822200019482
- Briant, R. M., and Bateman, M. D. (2009). Luminescence dating indicates radiocarbon age underestimation in late pleistocene fluvial deposits from eastern England. *J. Quaternary Sci.* 24 (8), 916–927. doi: 10.1002/jqs.1258
- Chen, G. (1984a). Quaternary fault block movement in chao-shan plain. *South China J. Of Seismology* 4 (4), 001–018. doi: 10.13512/j.hndz.1984.04.001
- Chen, W. (1984b). Several features for the development of sedimentary basin in chaoshan area, guangdong province. *South China J. Seismology* 4 (2), 20–30. doi: 10.13512/j.hndz.1984.02.004
- Cheng, P., Burr, G. S., Zhou, W., Chen, N., Hou, Y., Du, H., et al. (2020). The deficiency of organic matter ^{14}C dating in Chinese loess-paleosol sample. *Quaternary Geochronology* 56, 101051. doi: 10.1016/j.quageo.2019.101051
- Cheng, P., Dong, J., Zhou, W., Song, Y., Zhou, J., Fan, Y., et al. (2022). Paleoclimatic implications of ^{14}C age deviations in loess organic matter from xinjiang, Northwest China. *CATENA* 212, 106096. doi: 10.1016/j.catena.2022.106096
- Chen, H. W., Lee, T. Y., and Wu, L. C. (2010). High-resolution sequence stratigraphic analysis of late quaternary deposits of the changhua coastal plain in the frontal arc-continent collision belt of central Taiwan. *J. OF Asian Earth Sci.* 39 (3), 192–213. doi: 10.1016/j.jseaes.2010.02.009
- Gao, L., Long, H., Tamura, T., Hou, Y., and Shen, J. (2021). A~ 130 ka terrestrial-marine interaction sedimentary history of the northern jiangsu coastal plain in China. *Mar. Geology* 435, 106455. doi: 10.1016/j.margeo.2021.106455
- Goodfriend, G. A., and Stipp, J. J. (1983). Limestone and the problem of radiocarbon dating of land-snail shell carbonate. *Geology* 11 (10), 575–577. doi: 10.1130/0091-7613(1983)11<575:LATPOR>2.0.CO;2
- Guo, L., Wang, P., Zhang, K., Sheng, Q., Zhao, H., and Wang, C. (2013). OSL and ^{14}C ages of the late quaternary sediments in the east pearl river delta. *Geology China* 40 (6), 1842–1849.
- Hajdas, I., Ascough, P., Garnett, M. H., Fallon, S. J., Pearson, C. L., Quarta, G., et al. (2021). Radiocarbon dating. *Nat. Rev. Methods Primers* 1 (1), 62. doi: 10.1038/s43586-021-00058-7
- Hatté, C., Morvan, J., Noury, C., and Paterne, M. (2001). Is classical acid-alkali-treatment responsible for contamination? an alternative proposition. *Radiocarbon* 43 (2A), 177–182. doi: 10.1017/S003382220003798X
- Lai, Z. (2006). Testing the use of an OSL standardised growth curve (SGC) for de determination on quartz from the Chinese loess plateau. *Radiat. Measurements* 41 (1), 9–16. doi: 10.1016/j.radmeas.2005.06.031
- Lai, Z. (2010). Chronology and the upper dating limit for loess samples from luochuan section in the Chinese loess plateau using quartz OSL SAR protocol. *J. Asian Earth Sci.* 37 (2), 176–185. doi: 10.1016/j.jseaes.2009.08.003
- Lai, Z., and Brueckner, H. (2008). Effects of feldspar contamination on equivalent dose and the shape of growth curve for OSL of silt-sized quartz extracted from Chinese loess. *Geochronometria* 30 (1), 49–53. doi: 10.2478/v10003-008-0010-0
- Lai, Z., and Fan, A. (2014). Examining quartz OSL age underestimation for loess samples from luochuan in the Chinese loess plateau. *Geochronometria* 41 (1), 57–64. doi: 10.2478/s13386-013-0138-1
- Lai, Z., Mischke, S., and Madsen, D. (2014). Paleoenvironmental implications of new OSL dates on the formation of the “Shell bar” in the qaidam basin, northeastern qinghai-Tibetan plateau. *J. Paleolimnology* 51 (2), 197–210. doi: 10.1007/s10933-013-9710-1
- Lai, Z., and Ou, X. (2013). Basic procedures of optically stimulated luminescence (OSL) dating. *Prog. Geogr.* 32 (5), 683–693.
- Lai, Z.-P., and Wintle, A. G. (2006). Locating the boundary between the pleistocene and the Holocene in Chinese loess using luminescence. *Holocene* 16 (6), 893–899. doi: 10.1191/0959683606hol980rr
- Lai, Z., Wintle, A. G., and Thomas, D. S. (2007). Rates of dust deposition between 50 ka and 20 ka revealed by OSL dating at yuanbao on the Chinese loess plateau. *Palaeogeography Palaeoclimatology Palaeoecol.* 248 (3–4), 431–439. doi: 10.1016/j.palaeo.2006.12.013
- Li, P. R., Huang, Z. G., and Zong, Y. Q. (1988). New views on geomorphological development of the hanjiang river delta. *Acta Geographica Sin.* 55 (1), 19–34. doi: 10.11821/xb198801003
- Li, P., Huang, Z., Zong, Y., and Zhang, Z. (1987). *Hanjiang delta* (Beijing: Ocean Press).
- Ling, K., Zhu, S., Li, R., Lai, Z., and Wang, J. (2021). A new lithostratigraphic unit of Quaternary in Chaoshan plain—Paotai Formation. *J. Stratigraphy* 46 (01), 1–8. doi: 10.19839/j.cnki.dcxz.2021.0042
- Li, Y., Song, Y., Orozbaev, R., Dong, J., Li, X., and Zhou, J. (2020c). Moisture evolution in central Asia since 26 ka: Insights from a kyrgyz loess section, Western tian shan. *Quaternary Sci. Rev.* 249, 106604. doi: 10.1016/j.quascirev.2020.106604
- Liu, S. R. (1995). The divisions of guangdong province on new structure motion—also discussing the effect of new structure motion on coastline development. *Acta Scientiarum Naturalium Universitatis Sunyatseni* 34 (4), 93–99.
- Liu, K., and Lai, Z. P. (2012). Chronology of Holocene sediments from the archaeological salawusu site in the mu us desert in China and its palaeoenvironmental implications. *J. Asian Earth Sci.* 45, 247–255. doi: 10.1016/j.jseaes.2011.11.002
- Li, G., Wang, Z., Zhao, W., Jin, M., Wang, X., Tao, S., et al. (2020a). Quantitative precipitation reconstructions from chagan nur revealed lag response of East Asian summer monsoon precipitation to summer insolation during the Holocene in arid northern China. *Quaternary Sci. Rev.* 239, 106365. doi: 10.1016/j.quascirev.2020.106365
- Li, G., Yang, H., Stevens, T., Zhang, X., Zhang, H., Wei, H., et al. (2020b). Differential ice volume and orbital modulation of quaternary moisture patterns between central and East Asia. *Earth Planetary Sci. Lett.* 530, 115901. doi: 10.1016/j.epsl.2019.115901
- Long, Z., Wang, Z., Tu, H., Li, R., Wen, Z., Wang, Y., et al. (2022). OSL and radiocarbon dating of a core from the bohai Sea in China and implication for late quaternary transgression pattern. *Quaternary Geochronol.* 70, 101308. doi: 10.1016/j.quageo.2022.101308
- Madsen, D. B., Lai, Z., Sun, Y., Rhode, D., Liu, X., and Jeffrey Brantingham, P. (2014). Late quaternary qaidam lake histories and implications for a MIS 3 “Greatest lakes” period in northwest China. *J. Paleolimnology* 51 (2), 161–177. doi: 10.1007/s10933-012-9662-x
- Miller, G. H., and Andrews, J. T. (2019). Hudson Bay was not deglaciated during MIS-3. *Quaternary Sci. Rev.* 225, 105944. doi: 10.1016/j.quascirev.2019.105944
- Murray, A., Arnold, L. J., Buylaert, J.-P., Guérin, G., Qin, J., Singhvi, A. K., et al. (2021). Optically stimulated luminescence dating using quartz. *Nat. Rev. Methods Primers* 1 (1), 72. doi: 10.1038/s43586-021-00068-5
- Murray, A. S., and Olley, J. M. (2002). Precision and accuracy in the optically stimulated luminescence dating of sedimentary quartz: A status review. *Geochronometria* 21 (1), 1–16.
- Murray, A. S., and Wintle, A. G. (2000). Luminescence dating of quartz using an improved single-aliquot regenerative-dose protocol. *Radiat. measurements* 32 (1), 57–73. doi: 10.1016/S1350-4487(99)00253-X
- Nian, X., Zhang, W., Wang, Z., Sun, Q., Chen, J., Chen, Z., et al. (2018). The chronology of a sediment core from incised valley of the Yangtze river delta: Comparative OSL and AMS ^{14}C dating. *Mar. Geology* 395, 320. doi: 10.1016/j.margeo.2017.11.008
- Nilsson, M., Klarqvist, M., Bohlin, E., and Possnert, G. (2001). Variation in ^{14}C age of macrofossils and different fractions of minute peat samples dated by AMS. *Holocene* 11 (5), 579–586. doi: 10.1191/095968301680223521
- Ou, X., Lai, Z., Zhou, S., and Zeng, L. (2014). Timing of glacier fluctuations and trigger mechanisms in eastern qinghai-Tibetan plateau during the late quaternary. *Quaternary Res.* 81 (3), 464–475. doi: 10.1016/j.yqres.2013.09.007

- Palstra, S. W. L., Wallinga, J., Viveen, W., Schoorl, J. M., van den Berg, M., and van der Plicht, J. (2021). Cross-comparison of last glacial radiocarbon and OSL ages using periglacial fan deposits. *Quaternary Geochronology* 61, 101128. doi: 10.1016/j.quageo.2020.101128
- Pigati, J. S., Quade, J., Wilson, J., Jull, A. J. T., and Lifton, N. A. (2007). Development of low-background vacuum extraction and graphitization systems for ^{14}C dating of old (40–60ka) samples. *Quaternary Int.* 166 (1), 4–14. doi: 10.1016/j.quaint.2006.12.006
- Prescott, J. R., and Hutton, J. T. (1994). Cosmic ray contributions to dose rates for luminescence and ESR dating: large depths and long-term time variations. *Radiat. Measurements* 23 (2–3), 497–500. doi: 10.1016/1350-4487(94)90086-8
- Ramsey, C. B., and Lee, S. (2013). Recent and planned developments of the program OxCal. *Radiocarbon* 55 (2), 720–730. doi: 10.1017/S0033822200057878
- Reimer, P. J. (2012). Refining the radiocarbon time scale. *Science* 338 (6105), 337–338. doi: 10.1126/science.1228653
- Reimer, P. J., Austin, W. E. N., Bard, E., Bayliss, A., Blackwell, P. G., Bronk Ramsey, C., et al. (2020). The IntCal20 northern hemisphere radiocarbon age calibration curve (0–55 cal kBP). *Radiocarbon* 62 (4), 725–757. doi: 10.1017/rdc.2020.41
- Rhodes, E. J. (2011). Optically stimulated luminescence dating of sediments over the past 200,000 years. *Annu. Rev. Earth Planetary Sci.* 39, 461–488. doi: 10.1146/annurev-earth-040610-133425
- Roberts, H., and Duller, G. A. (2004). Standardised growth curves for optical dating of sediment using multiple-grain aliquots. *Radiat. Measurements* 38 (2), 241–252. doi: 10.1016/j.radmeas.2003.10.001
- Roberts, H., and Wintle, A. (2003). Luminescence sensitivity changes of polymineral fine grains during IRSL and [post-IR] OSL measurements. *Radiat. Measurements* 37 (6), 661–671. doi: 10.1016/S1350-4487(03)00245-2
- Rohling, E. J., Grant, K., Hemleben, C., Siddall, M., Hoogakker, B., Bolshaw, M., et al. (2008). High rates of sea-level rise during the last interglacial period. *Nat. Geosci.* 1 (1), 38–42. doi: 10.1038/ngeo.2007.28
- Singarayer, J., and Bailey, R. (2003). Further investigations of the quartz optically stimulated luminescence components using linear modulation. *Radiat. Measurements* 37 (4–5), 451–458. doi: 10.1016/S1350-4487(03)00062-3
- Song, Y., Chen, W., Pan, H., Zhang, Z., He, Z., Chen, X., et al. (2012). Geological age of quaternary series in lianjiang plain. *J. Jilin Univ.(Earth Sci. Ed.)* 42, 154–161. doi: 10.13278/j.cnki.jjuese.2012.s1.040
- Song, Y., Lai, Z., Li, Y., Chen, T., and Wang, Y. (2015). Comparison between luminescence and radiocarbon dating of late quaternary loess from the ili basin in central Asia. *Quaternary Geochronology* 30, 405–410. doi: 10.1016/j.quageo.2015.01.012
- Stanley, D. J., and Chen, Z. (2000). Radiocarbon dates in china's Holocene Yangtze delta: record of sediment storage and reworking, not timing of deposition. *J. Coast. Res.* 16 (4), 1126–1132. Available at: <http://www.jstor.org/stable/4300129>
- Sun, Y., Lai, Z., Madsen, D., and Hou, G. (2012). Luminescence dating of a hearth from the archaeological site of jiangxigou in the qinghai lake area of the northeastern qinghai-Tibetan plateau. *Quaternary Geochronology* 12, 107–110. doi: 10.1016/j.quageo.2012.01.010
- Sun, J.-L., Xu, H. L., Wu, P., Wu, Y.-B., Qiu, X.-L., and Zhan, W.-H. (2007). Late quaternary sedimentological characteristics and sedimentary environment evolution in sea area between nan'ao and chenghai, eastern guangdong. *J. Trop. Oceanogr.* 26, 30–36.
- Tang, Y., Zheng, Z., Chen, C., Wang, M., and Chen, B. (2018). Evolution of the lian river coastal basin in response to quaternary marine transgressions in southeast China. *Sedimentary Geology* 366, 1–13. doi: 10.1016/j.sedgeo.2018.01.003
- Väliiranta, M., Oinonen, M., Seppä, H., Korkkonen, S., Juutinen, S., and Tuittila, E.-S. (2014). Unexpected problems in AMS ^{14}C dating of fen peat. *Radiocarbon* 56 (1), 95–108. doi: 10.2458/56.16917
- Wallinga, J., and Cunningham, A. C. (2015). "Luminescence dating, uncertainties and age range," in *Encyclopedia of scientific dating methods* (Netherlands: Springer), 440–445.
- Wang, Y., Chen, T. E. C., An, F., Lai, Z., Zhao, L., et al. (2018b). Quartz OSL and K-feldspar post-IR IRSL dating of loess in the huangshui river valley, northeastern Tibetan plateau. *Aeolian Res.* 33, 23–32. doi: 10.1016/j.aeolia.2018.04.002
- Wang, Z., Zhao, H., Dong, G., Zhou, A., Liu, J., and Zhang, D. (2014). Reliability of radiocarbon dating on various fractions of loess-soil sequence for dadiwan section in the western Chinese loess plateau. *Front. Earth Sci.* 8 (4), 540–546. doi: 10.1007/s11707-014-0431-1
- Wang, M., Zheng, Z., Gao, Q., Zong, Y., Huang, K., and Shi, S. (2018a). The environmental conditions of MIS5 in the northern south China Sea, revealed by n-alkanes indices and alkenones from a 39 m-long sediment sequence. *Quaternary Int.* 479, 70–78. doi: 10.1016/j.quaint.2017.08.026
- Wang, M. Y., Zheng, Z., Huang, K. Y., Zong, Y. Q., Liu, Z. H., Peng, Z. L., et al. (2016). U-37(K⁺) temperature estimates from eemian marine sediments in the southern coast of hainan island, tropical China. *J. OF Asian Earth Sci.* 127, 91–99. doi: 10.1016/j.jseae.2016.06.021
- Wang, J. H., Zheng, Z., and Wu, C. Y. (1997). Sedimentary facies and paleoenvironmental evolution of the late quaternary in the chaoshan plain, East guangdong. *Acta Scientiarum Naturalium Universitatis Sunyatseni* 36 (1), 95–100.
- Wintle, A. G., and Murray, A. S. (2006). A review of quartz optically stimulated luminescence characteristics and their relevance in single-aliquot regeneration dating protocols. *Radiat. Measurements* 41 (4), 369–391. doi: 10.1016/j.radmeas.2005.11.001
- Xie, Y., Wang, Q., Long, G., Zhou, Y., Zheng, Z., and Huang, X. (2014). Transgressive sequence since the late pleistocene in xiaolan town-wanqingsha area, zhujiang river estuary. *J. Palaeogeogr.* 16, 835–852. doi: 10.7605/gdxb.2014.06.067
- Xu, X., Li, H., Tang, L., Lai, Z., Xu, G., Zhang, X., et al. (2020). Chronology of a Holocene core from the pearl river delta in southern China. *Front. Earth Sci.* 8 (262). doi: 10.3389/feart.2020.00262
- Xu, Y., Tian, T., Shen, Q., Luo, L., and Lai, Z. (2021). Late quaternary aggradation of the datong basin in northern China revealed by OSL dating of core sediments and implications for groundwater arsenic pollution. *Catena* 207, 105650. doi: 10.1016/j.catena.2021.105650
- Xu, X., Zhong, J., Huang, X., Li, H., Ding, Z., and Lai, Z. (2022). Age comparison by luminescence using quartz and feldspar on core HPQK01 from the pearl river delta in China. *Quaternary Geochronol.* 71, 101320. doi: 10.1016/j.quageo.2022.101320
- Yi, L., Lai, Z., Yu, H., Xu, X., Su, Q., Yao, J., et al. (2013). Chronologies of sedimentary changes in the south bohai sea, china: constraints from luminescence and radiocarbon dating. *Boreas* 42 (2), 267–284. doi: 10.1111/j.1502-3885.2012.00271.x
- Yim, W.-S., Ivanovich, M., and Yu, K.-F. (1990). Young age bias of radiocarbon dates in pre-Holocene marine deposits of Hong Kong and implications for pleistocene stratigraphy. *Geo-Marine Lett.* 10 (3), 165–172. doi: 10.1007/BF02085932
- Yokoyama, Y., Esat, T. M., and Lambeck, K. (2001). Coupled climate and sea-level changes deduced from huon peninsula coral terraces of the last ice age. *Earth Planetary Sci. Lett.* 193 (3–4), 579–587. doi: 10.1016/S0012-821X(01)00515-5
- Zhang, K., Ling, K., Liu, C., Yin, J., and Wu, Y. (2020). Holocene Diatom records in the rongjiang plain and implications for palaeoenvironmental changes. *Acta Scientiarum Naturalium Universitatis Sunyatseni* 59 (03), 32–42. doi: 10.13471/j.cnki.acta.snus.2020.03.004
- Zhang, Y., and Shi, Y. (1989). Problems in Carbon-14 dating of Marine Sediments. *Mar. Sci.* (2), 28–32.
- Zhao, J., Yin, X., Harbor, J. M., Lai, Z., Liu, S., and Li, Z. (2013). Quaternary glacial chronology of the kanas river valley, Altai mountains, China. *Quaternary Int.* 311, 44–53. doi: 10.1016/j.quaint.2013.07.047
- Zheng, Z., and Li, Q. (2000). Vegetation, climate, and sea level in the past 55,000 years, hanjiang delta, southeastern China. *Quaternary Res.* 53 (3), 330–340. doi: 10.1006/qres.1999.2126
- Zhou, Y. (2008). Primary geological hazards to the continental coast in shantou. *Trop. Geogr.* 28 (4), 331–337. doi: 10.13284/j.cnki.rddl.001168
- Zong, Y. Q. (1987). Depositional cycles of the Quaternary in the Hanjiang delta. *Trop. Geogr.* 7 (2), 117–126.
- Zong, Y., Huang, G., Li, X. Y., and Sun, Y. Y. (2015). Late Quaternary tectonics, sea-level change and lithostratigraphy along the northern coast of the South China Sea. *Geological Soc. London Special Publications* SP429, 421. doi: 10.1144/SP429.1